IFAC Workshop on Adaptation and Learning in Control and
Signal Processing, and IFAC Workshop on Periodic Control
Systems, Yokohama, Japan, August 30 – September 1, 2004

THE WINDSURFER APPROACH TO ITERATIVE CONTROL AND IDENTIFICATION USING AN $\mathcal{H}_\infty$ ALGORITHM

Arvin Dehghani *,**,[1] **Alexander Lanzon** *,**
Brian D. O. Anderson *,**

* *Department of Systems Engineering,*
Research School of Information Sciences and Engineering,
The Australian National University, ACT 0200, Australia
** *National ICT Australia Ltd., Locked Bag 8001,*
Canberra, ACT 2601, Australia [2]

Abstract: The windsurfing approach to iterative control entails several controller designs to gradually and safely widen the closed-loop bandwidth. Eventually some validation tests are carried out in order to stop the algorithm. In this paper, an $\mathcal{H}_\infty$ design algorithm is presented in order to remove the empirical aspect from the stopping criteria and to make the procedure more systematic, hence expediting the design. Furthermore, a new controller design method is introduced which relaxes some restrictive assumptions on the plant model and tackles well some issues with the controller design step. This enables us to address a wider class of practical problems.

Keywords: *Windsurfer Approach; Adaptive Control; Robust Control*

1. INTRODUCTION

One of the model-based iterative identification and control design methods, *the windsurfer approach*, was first introduced in (Anderson and Kosut, 1991). This proposes an iterative algorithm which gradually broadens the bandwidth of a closed-loop system through repetition of a two-step procedure using identification and controller re-design steps. Hence, the algorithm, outlined e.g. in (Lee *et al.*, 1993) and (Anderson, 2002), is constructed to achieve the desired performance and design objectives, in which the Internal Model Control (IMC) method (Morari and Zafiriou, 1989) is iteratively utilised in the controller design steps. In the case of *stable* plants, the IMC design method offers the advantage of simplicity and the fact that the closed-loop bandwidth of the system can be set via a single design parameter (Lee *et al.*, 1993). However, if the plant is *unstable*, the same simple IMC design method cannot be used. Treatment of the unstable plant case can be found in papers (Lee *et al.*, 2001) and (Campi *et al.*, 1982). Nevertheless, there are some inadequacies with the IMC design methods for both stable and unstable plants which will be extensively discussed and addressed in section 2.

In this paper, we introduce a modified algorithm for the windsurfer approach in section 3 by incorporating a new controller design method. This new controller design method (section 2.2) maintains the desirable features of the IMC design method, but also extends its applicability and addresses some of the IMC shortcomings. The proposed algorithm introduces an $\mathcal{H}_\infty$ design technique in order to make the windsurfer approach more systematic and to relax some restrictive assumptions on the plant.

[1] Corresponding author. *Arvin.Dehghani@anu.edu.au, Fax: (61)-2-6125 8660*
[2] This work was supported by an ARC Discovery-Projects Grant (DP0342683) and National ICT Australia. National ICT Australia is funded through the Australian Government's *Backing Australia's Ability* initiative, in part through the Australian Research Council.

2. CONTROLLER DESIGN METHOD

Internal Model Control is a simple but effective control design method which has been successfully used in many applications where a desired closed-loop amplitude response from reference to plant output must be achieved. Furthermore, for a *stable* plant, adjustment of a single parameter directly and simply determines the closed-loop bandwidth and hence the reference tracking capabilities.

2.1 Difficulties with the IMC approach

Consider the feedback system in Fig. 1. One can express y and u in terms of r_1 and r_2 as follows:

$$\begin{bmatrix} y \\ u \end{bmatrix} = H(P_i, C_i) \begin{bmatrix} r_1 \\ r_2 \end{bmatrix} = \begin{bmatrix} \frac{P_i C_i}{1+P_i C_i} & \frac{P_i}{1+P_i C_i} \\ \frac{C_i}{1+P_i C_i} & \frac{1}{1+P_i C_i} \end{bmatrix} \begin{bmatrix} r_1 \\ r_2 \end{bmatrix} \quad (1)$$

where r_2 represents a second external input or disturbance acting on the plant input. To motivate the importance of considering the four transfer functions in equation (1), let us note some key points. The (1,1) transfer function $T_{yr_1} = \frac{P_i C_i}{1+P_i C_i}$ is clearly important for reference tracking and the IMC design method deals particularly with this. Special care, however, must be exercised in regard to the other three transfer functions as the IMC (Morari and Zafiriou, 1989) does not handle them explicitly. For a sensible design, the transfer function from plant input disturbance to output, $T_{yr_2} = \frac{P_i}{1+P_i C_i}$, must be maintained below a certain size since we wish plant input disturbances to be attenuated at the plant output. Likewise, $T_{ur_1} = \frac{C_i}{1+P_i C_i}$ represents the transfer function from reference input to control signal and hence, must be kept below a certain size in order to avoid control actuator saturation and high energy control action. Furthermore, the size of the four transfer functions in equation (1) is related to a generalised robust stability margin (Vinnicombe, 2000) which corresponds to the amount of (coprime factor) uncertainty that can perturb P_i without destabilising the loop (Zhou *et al.*, 1996). With this introduction in mind, let us now record the circumstances where the IMC design method described in (Morari and Zafiriou, 1989) cannot be properly used or is limited by restrictive assumptions.

(a) If P_i is unstable, then the simple IMC design method for the stable case outlined in (Morari and Zafiriou, 1989) cannot be used. There does exist a different IMC design method for the unstable plant case but the procedure is much more complicated (see (Lee *et al.*, 2001; Campi *et al.*, 1982));

(b) If P_i has zeros on the $j\omega$-axis, then the factoring of P_i into stable all-pass, $[P_i]_a$, and stable strictly minimum-phase, $[P_i]_m$, components as required by (Morari and Zafiriou, 1989) is not possible.

(c) If the model has lightly-damped stable poles in the closed-loop passband, then $\frac{P_i}{1+P_i C_i}$ will have large gain near the frequencies of those poles;

(d) If the model has lightly-damped stable or unstable zeros in the closed-loop passband, then $\frac{C_i}{1+P_i C_i}$ will have large gain near the frequencies of those zeros;

(e) If the bandwidth of the IMC filter F_i (Morari and Zafiriou, 1989) is much larger than the bandwidth of P_i, then $|C_i|$ will be very large at frequencies inside the bandwidth of F_i and outside the bandwidth of P_i, and again the control signal will be very large;

(f) If the roll-off rate of F_i is desired to be less than the roll-off rate of P_i, then the IMC design method outlined in (Morari and Zafiriou, 1989) will result in an improper controller, C_i.

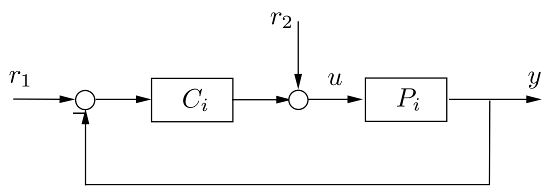

Fig. 1. Standard Feedback Configuration

Notice that the IMC design method described in (Morari and Zafiriou, 1989) fails and cannot be used in situations (a), (b),(f). However, the IMC design method can be applied in situations (c),(d) and (e) but difficulties may occur. In the sequel, we shall introduce a new controller design method that inherits the useful desired features of the IMC design method, but addresses problems stated in situations (a)–(f) explicitly.

2.2 Proposed $\mathcal{H}_\infty$ Controller Design Method

On the one hand, we would like to utilise the desired features of the IMC on either a stable or unstable plant. On the other hand, we would like to ensure that the magnitudes of all the transfer function matrix entries in equation (1) do not become too large. These two objectives, however, are not the same and we need to reformulate the problem in such a way to capture our objectives. Therefore, we shall introduce an $\mathcal{H}_\infty$ index and require this index to be minimised over all stabilising controllers. We normally have performance objectives in mind, which requires some transfer functions to be small or below certain values in some frequency regions and other transfer functions small or below certain values at other frequencies. The $\mathcal{H}_\infty$ index will be weighted to achieve the desired effect. Let us outline our proposed controller design method:

(i) Given a model of the plant, P_i do the following factorisation:

$$P_i = [P_i]_a [P_i]_m \; ; \begin{cases} [P_i]_a \in \mathcal{RH}_\infty \; , \; [P_i]_a^{\sim} [P_i]_a = I \\ [P_i]_m \;\; has\ no\ zeros\ in\ \mathbb{C}_+ \end{cases} \quad (2)$$

where $\mathbb{C}_+$ denotes the open right-half plane.

(ii) The admissible controller is given by solving the following $\mathcal{H}_\infty$ problem:

$$\gamma_i = \min_{C_i \in \underline{\mathcal{C}}} \left\| \begin{matrix} \frac{P_iC_i}{1+P_iC_i} - [P_i]_a F_i & \epsilon_2(s)\frac{P_i}{1+P_iC_i} \\ \epsilon_1(s)\frac{C_i}{1+P_iC_i} & \epsilon_1(s)\epsilon_2(s)\frac{1}{1+P_iC_i} \end{matrix} \right\|_\infty \quad (3)$$

where $\underline{\mathcal{C}}$ denotes the set of all proper stabilising controllers for the plant, P_i, and $\epsilon_1(s)$ and $\epsilon_2(s)$ are SISO, stable, minimum-phase and proper weights [3]. We shall explain in detail the selection of the weighting functions in the following section.

One can easily verify that this proposed design method addresses all the aforestated difficulties, cases (a)–(f), with the IMC design method.

2.3 Design of weighting functions $\epsilon_1(s)$ and $\epsilon_2(s)$

The weighting functions were introduced as a part of the $\mathcal{H}_\infty$ index in equation (3) and we shall now discuss the way to design them. One should realize that, based upon the particular application specifications and also the characteristics of the plant, we will have different objectives in different frequency regions. Let us now set out our design objectives, as specified in index (3):

(1) Let α be the desired closeness between $\frac{P_iC_i}{1+P_iC_i}$ and $[P_i]_aF_i$ in an $\mathcal{H}_\infty$ sense. That is, we require $\left\|\frac{P_iC_i}{1+P_iC_i} - [P_i]_aF_i\right\|_\infty \leq \alpha$.

(2) Let β_p be the maximum tolerable gain in the appropriate frequency region for the transfer function $T_{yr_2} = \frac{P_i}{1+P_iC_i}$. That is, we require $\bar{\sigma}\left[\frac{P_i}{1+P_iC_i}(j\omega)\right] \leq \beta_p \qquad \forall\omega \in [\omega_1, \omega_2]$.

(3) Let β_c be the maximum tolerable gain in the appropriate frequency region for the transfer function $T_{ur_1} = \frac{C_i}{1+P_iC_i}$. That is, we require $\bar{\sigma}\left[\frac{C_i}{1+P_iC_i}(j\omega)\right] \leq \beta_c \qquad \forall\omega \in [\omega_3, \omega_4]$.

Now, we have three different numbers, i.e. α, β_p and β_c, that capture our objectives. These three numbers will be used to specify $\epsilon_1(s)$ and $\epsilon_2(s)$ as we discuss next. Once $\epsilon_1(s)$ and $\epsilon_2(s)$ are specified, we just need to check the number γ_i to determine whether the design was successful in achieving our objectives or not. Towards this end, note that the index in (3) certainly guarantees that:

$$\bar{\sigma}\left[\frac{P_iC_i}{1+P_iC_i} - [P_i]_aF_i\right] \leq \gamma_i \qquad \forall\omega \quad , \quad (4)$$

$$\bar{\sigma}\left[\frac{P_i}{1+P_iC_i}(j\omega)\right] \leq \frac{\gamma_i}{|\epsilon_2(j\omega)|} \qquad \forall\omega \quad , \quad (5)$$

$$\bar{\sigma}\left[\frac{C_i}{1+P_iC_i}(j\omega)\right] \leq \frac{\gamma_i}{|\epsilon_1(j\omega)|} \qquad \forall\omega \quad (6)$$

are achieved. Let us consider four different scenarios that describe how $\epsilon_1(j\omega)$ and $\epsilon_2(j\omega)$ ought to be chosen.

[3] Note that $\min_{C_i \in \underline{\mathcal{C}}} \|\mathcal{F}_l(.,.)\|_\infty$ rather than $\inf_{C_i \in \underline{\mathcal{C}}} \|\mathcal{F}_l(.,.)\|_\infty$ is used since we need both γ_i and $C_i \in \underline{\mathcal{C}}$.

2.3.1. ***If*** $\epsilon_1(j\omega) = 0$ ***and*** $\epsilon_2(j\omega) = 0$, then the $\mathcal{H}_\infty$ index specified in equation (3) reduces to

$$\gamma_i = \min_{C_i \in \underline{\mathcal{C}}} \left\|\frac{P_iC_i}{1+P_iC_i} - [P_i]_aF_i\right\|_\infty \quad (7)$$

and hence C_i will be exactly the standard IMC controller [4], at least if P_i is stable and has no $j\omega$-axis zeros and all other assumptions of the IMC design method outlined in (Morari and Zafiriou, 1989) are fulfilled (i.e. $\gamma_i = 0$ for such a case) [5]. Thus, $\epsilon_1(j\omega)$ and $\epsilon_2(j\omega)$ can be set to be very small in the frequency regions where the plant characteristics and our performance objectives are such that an IMC controller can perform well at those frequencies.

2.3.2. ***If*** $\epsilon_1(j\omega) = 0$ ***but*** $\epsilon_2(j\omega) \neq 0$, then it is clear that, in this situation, we are trying to make $\frac{P_iC_i}{1+P_iC_i}$ close to $[P_i]_aF_i$ but simultaneously we are seeking to limit the size of $\frac{P_i}{1+P_iC_i}$. With reference to section 2.1, we choose $|\epsilon_2(j\omega)| \geq \frac{\alpha}{\beta_p}$ near the frequencies of the lightly-damped poles of P_i, as this will then limit the size of $\frac{P_i}{1+P_iC_i}$.

2.3.3. ***If*** $\epsilon_1(j\omega) \neq 0$ ***but*** $\epsilon_2(j\omega) = 0$, then it is clear that, in this situation, we are trying to make $\frac{P_iC_i}{1+P_iC_i}$ close to $[P_i]_aF_i$ but limit the size of $\frac{C_i}{1+P_iC_i}$. With reference to section 2.1, we choose $|\epsilon_1(j\omega)| \geq \frac{\alpha}{\beta_c}$ near the frequencies of the lightly-damped zeros of P_i, as this will limit the size of $\frac{C_i}{1+P_iC_i}$.

2.3.4. ***If*** $\epsilon_1(j\omega) \neq 0$ ***and*** $\epsilon_2(j\omega) \neq 0$, then we can trade-off the closeness requirement of $\frac{P_iC_i}{1+P_iC_i}$ to $[P_i]_aF_i$ with limiting the size of both $\frac{P_i}{1+P_iC_i}$ and $\frac{C_i}{1+P_iC_i}$ at the appropriate frequencies. Again, $\epsilon_1(j\omega)$ and $\epsilon_2(j\omega)$ are chosen such that $|\epsilon_1(j\omega)| \geq \frac{\alpha}{\beta_c}$ and $|\epsilon_2(j\omega)| \geq \frac{\alpha}{\beta_p}$ at the right frequencies.

3. NEW WINDSURFER DESIGN METHOD

The iterative control and identification approach to adaptive control includes two types of steps: identification and controller design steps. With a stabilising controller acting on the true plant, a model of the plant is identified through a closed-loop identification procedure.

As mentioned in the introduction, the originally proposed windsurfer approach to iterative identification and control re-design (Lee *et al.*, 1993)

[4] Note though that the $\mathcal{H}_\infty$ index can be used even if the plant, P_i, is unstable or has $j\omega$-axis zeros, although γ_i may not be equal to zero in this case.

[5] The minimum may not be attainable when P_i is unstable or has $j\omega$-axis zeros or the roll-off rate of F is smaller than that of P_i in which case there would be an infimum but not a minimum.

gradually and safely increases the closed-loop bandwidth using the IMC design method at the control stage. As extensively discussed in section 2.1, the IMC design method suffers from some serious deficiencies. These are, however, all addressed in our new $\mathcal{H}_\infty$ design method (see section 2.2). Hence, in the sequel, we shall propose a *modified* windsurfer algorithm that makes use of our new $\mathcal{H}_\infty$ design method, instead of the IMC, at the control design step. Because of this change, we modify other parts of the windsurfer algorithm to make it more amenable to our design method. It is important to understand that our new $\mathcal{H}_\infty$ design method is better suited to flag when the re-identification is required, when compared to the IMC design method, as will become evident below.

3.1 A Modified Iterative Identification and Controller Re-design Algorithm

Given a true physical plant, P_t, which is unknown, and a known controller, C_0, which stabilises P_t, the algorithm follows the steps outlined below.

- **Step 1.** Perform the closed-loop identification, outlined in (Anderson, 2002) and the references therein, so that the identified plant model P_i satisfies: $[P_i, C_i]$ stable and
$$\max_{1\le k\le N} \bar{\sigma}[H(P_t, C_i) - H(P_i, C_i)\ (j\omega_k)]$$
small[6].
- **Step 2.** Set an initial bandwidth, λ_0, for the desired closed-loop response, $F_i(j\omega)$. The initial bandwidth can be chosen to be much smaller than that of the identified model where its magnitude response is flat. It is always safe to choose the initial bandwidth of $F_i(j\omega)$ to be an order of magnitude less than the lowest predominant feature of $P_i(j\omega)$. That is, if there is a resonant pole at ω_0 inside the plant bandwidth, choose the initial bandwidth for $F_i(j\omega)$ to be $\frac{\omega_0}{10}$;
- **Step 3.** Find the critical frequency regions in P_i based on the cases, (a) – (f), discussed in section 2.1. Based on the desired closed-loop objectives and specifications, set:
  (a) the positive number α in the sense that $\left\| \frac{P_i C_i}{1+P_i C_i} - [P_i]_a F_i \right\|_\infty \le \alpha$.
  (b) the positive numbers β_p and β_c in the sense that $\begin{cases} \bar{\sigma}\left[\frac{P_i}{1+P_i C_i}(j\omega)\right] \le \beta_p & \forall\omega \in [\omega_1, \omega_2] \\ \bar{\sigma}\left[\frac{C_i}{1+P_i C_i}(j\omega)\right] \le \beta_c & \forall\omega \in [\omega_3, \omega_4] \end{cases}$
- **Step 4.** Design the frequency weights, $\epsilon_1(s)$ and $\epsilon_2(s)$, according to the rules given in section 2.3, using the specified values α, β_p and β_c in **Step 3**, for the appropriate frequency regions;

[6] It can be shown that if $[P_t, C_i]$ and $[P_i, C_i]$ are stable then for SISO systems $\bar{\sigma}\,[H(P_t, C_i) - H(P_i, C_i)] = \left[\,|C_i| + \frac{1}{|C_i|}\right]\,\left|\frac{P_t C_i}{1+P_t C_i} - \frac{P_i C_i}{1+P_i C_i}\right|$.

- **Step 5.** Solve the $\mathcal{H}_\infty$ controller design problem given in equation (3) and obtain γ_i and C_i;
- **Step 6.** If $\gamma_i \le \alpha$ and $\max_{1\le k\le N} \bar{\sigma}[H(P_t, C_i) - H(P_i, C_i)\ (j\omega_k)]$ is small, then increase the bandwidth for F_i by 10%; and go to **Step 5**. Otherwise, go to **Step 7**;
- **Step 7.** Discard the last controller. IF there was a previous controller, then go to **Step 1**, else **END**.

4. NUMERICAL EXAMPLE

In this section, we consider a plant which is examined in (Lee *et al.*, 1993) and (Anderson, 2002) in order to discuss the proposed algorithm and also to show its systematic easy-to-use features.

The true plant is a robot arm with the transfer function[7], $P_t(s) = 0.5196 \frac{\prod_{i=1}^{5}(s-z_i)}{\prod_{i=1}^{6}(s-p_i)}$ where the zeros are -13.162, $-10.646 \pm j12.27$, $7.169 \pm j11.54$ and the poles are $-0.0996 \pm j3.0017$, $-0.3339 \pm j12.131$, $-1.8450 \pm j31.481$.

We shall apply the algorithm described in section 3.1 and use the closed-loop identification procedure detailed in (Hansen, 1989) and outlined in (Anderson, 2002). To start, the identification procedure requires an initial model of the plant and a controller that stabilises both the model and the true plant. The initial model P_0, obtained from (Lee *et al.*, 1995), and the controller C_0, standard IMC controller to achieve a closed-loop bandwidth of 0.1 rad/s, are chosen to be

$$P_0 = \frac{0.1709(s+13.31)}{s^2+0.1806s+9.024},\ C_0 = \frac{0.5849(s^2+0.1806s+9.024)}{s(s+13.31)}.$$

Using the identification procedure of (Hansen, 1989), we identify a model $\tilde{P}_1$ using P_0 and C_0 and the identification data collected. The (reference) input is chosen to consist of four periods of a zero-mean square wave of amplitude 1. The plant output was corrupted by zero-mean white noise with standard deviation of 0.05. The Numerical Subspace-Based State Space Model Estimation N4SID (built in MATLAB function) is used to estimate the model. Choosing the identified Youla-Kucera parameter R (discussed in (Anderson, 2002)) to be of order five, the resulting identified model, $\tilde{P}_1$, is of degree eleven and is given by $\tilde{P}_1(s) = 0.51819 \frac{1.0\times10^2 \prod_{i=1}^{7}(s-z_i)}{1.0\times10^2 \prod_{i=1}^{8}(s-p_i)}$ where the zeros are -0.0038, -0.1331, -8.9357, -0.0043, $0.0628 \pm j0.1300$, $-0.0658 \pm j0.0802$, $-0.1573 \pm j0.0109$ and the poles are -0.0039, -0.0041, -8.9357, $-0.0297 \pm j0.3068$, $-0.0070 \pm j0.1180$, $-0.1130 \pm j0.0030$, $-0.0009 \pm j0.0300$.

For this identified plant model $\tilde{P}_1$, $\max_{1\le k\le N} \bar{\sigma}[H(P_t, C_0) - H(\tilde{P}_1, C_0)\ (j\omega_k)] = 0.4683$. Although one may think that 0.4683 is not small enough, we point out

[7] Note that, the windsurfer approach does not have available to it the mathematical description of the true plant; we only use this information to verify the method.

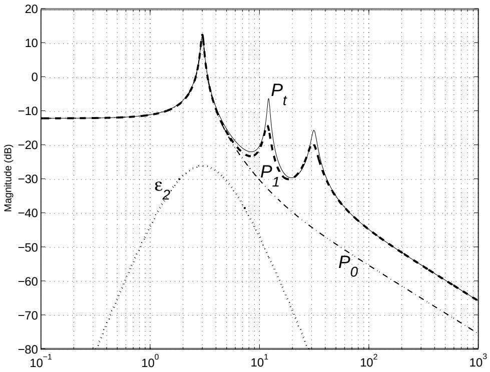

Fig. 2. Magnitude Responses of P_t, P_0, P_1, and ϵ_2

that (a) for the identified model G_1 in (Lee *et al.*, 1995) $\max_{1 \le k \le N} \bar{\sigma}[H(P_t, C_i) - H(G_1, C_i)\ (j\omega_k)] = 0.8637$ so our scheme is no worse; (b) it is very difficult for identification schemes to pick out the detailed resonant structures of an unknown true plant, and typically the largest identification errors occur at or near these resonances.

To avoid degree explosion in the identified model, we employ the closed-loop model reduction method detailed in section 4.3 (pp 137–140) of reference (Obinata and Anderson, 2001). The Hankel singular values of the graph symbols of $\tilde{P}_1$ are $2.1976,\ 2.0657,\ 1.5216,\ 0.11324,\ 0.1191,\ 0.0801,\ 0.0552,\ 0.0460,\ 0.0002,\ 2.84e-5,\ 7.38e-10$. We perform balanced realization and the result is truncated to retain all Hankel singular values greater than $0.01\,\sigma_1$. The identified plant P_1 is stabilised by C_0, and we estimate $\max_{1 \le k \le N} \bar{\sigma}[H(P_t, C_0) - H(P_1, C_0)\ (j\omega_k)] = 0.4684$. The magnitude responses of the true plant $P_t(j\omega)$ and the model $P_1(j\omega)$ are shown in Fig. 2.

The initial bandwidth, λ_1 is set to 0.1, which is much smaller than that of P_1 and is well below the first resonant frequency. We divide (section 2.3) the plant model frequency response into two regions; *region 1:* below 1.5 rad/s, and *region 2:* contains the frequencies around the first resonant mode. We shall now set our closed-loop performance objectives to be: (i) $\alpha = 0.1$; (ii) $\beta_p = 2$ ($\approx 6\,dB$). Here, the closed-loop bandwidth λ_1 lies in the *first region*, hence $\epsilon_1(j\omega)$ is set to be small (say 0.001), and $\epsilon_2(j\omega)$ is chosen to take care of the first resonant mode of P_1 at $3rad/s$; $\epsilon_2(j\omega)$ is set, Fig. 2, to have the maximum gain of $-26\,dB$, ($\alpha/\beta_p = 0.1/2 = 0.05$).

As stated in **Step 5** of our algorithm, we then solve the $\mathcal{H}_\infty$ index in equation (3) with $F_1 = \frac{\lambda_1}{s+\lambda_1}$ and the controller obtained achieves the norm value of 0.10 ($\gamma_1 = 0.10 \le \alpha$). The second condition in **Step 6** of our algorithm, $\max_{1 \le k \le N} \bar{\sigma}[H(P_t, C_0) - H(P_1, C_0)\ (j\omega_k)] = 0.3136$. The two conditions of **Step 6** are met until we push out the bandwidth to $\lambda_i = 1.0$ where $\gamma_i = 0.09 < \alpha$ but the second condition is not satisfied since the norm has increased to a value (0.4698) greater than the initial one (0.4684). This points out that re-identification is necessary. Therefore, we discard the last controller and go back to **Step 1** for re-identification.

After re-identification, we can gradually (10% in each iteration) increase the closed-loop bandwidth λ_i to 8.2 rad/s where both conditions of **Step 6** are not satisfied and hence re-identification is required.

We perform the re-identification again and then set our closed-loop performance objectives to be: (i)$\alpha = 0.1$; (ii) $\beta_p = 2$ ($\approx 6\,dB$); (iii) $\beta_c = 30$ ($\approx 30\,dB$). The frequency cost $\epsilon_1(j\omega)$ is chosen to gradually reach the maximum gain of almost $-50\,dB$ ($\alpha/\beta_c = 0.1/30$) at $4rad/s$, where the plant model loses its bandwidth to the controller. The cost $\epsilon_2(j\omega)$ is chosen to be the same as before (Fig. 3). Now, The closed-loop bandwidth can be further pushed out to 11.2 rad/s. After re-identification, the bandwidth can not be increased more than 11.2 rad/s as γ_i will be more than 0.1 and the performance objectives will not be met.

Let us now record a number of key attributes which make our proposed algorithm much more suitable for the windsurfer approach. The results in (Lee *et al.*, 1995) show that the closed-loop bandwidth can be expanded to 12 rad/s whereas ours can be expanded to 11.2 rad/s. Considering the 4-block transfer function $H(G_1, C_{IMC})$, where G_1 denotes the identified model in (Lee *et al.*, 1995) and C_{IMC} refers to the controller which was designed to achieve the close-loop bandwidth of 12 rad/s, we note the following important points:

- the magnitude response of the transfer function $\frac{G_1 C_{IMC}}{1+G_1 C_{IMC}}$ is exactly specified by the IMC filter $F = \frac{12}{(s+12)^2}$ and hence exact reference tracking is achieved for the desired bandwidth on the identified model. However, $\max_{1 \le k \le N} \bar{\sigma}[\frac{P_t C_{IMC}}{1+P_t C_{IMC}} - \frac{G_1 C_{IMC}}{1+G_1 C_{IMC}}\ (j\omega_k)] = 0.57$ which indicates a large discrepancy in reference

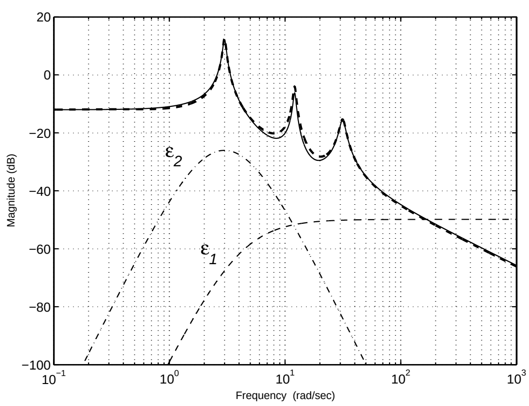

Fig. 3. Magnitude Responses of P_t, P_3, ϵ_1 and ϵ_2

tracking capabilities if C_{IMC} is chosen to be used on the true plant. On the contrary, our proposed algorithm ensures

$$\max_{1\leq k\leq N} \bar{\sigma}[\frac{P_t C_i}{1+P_t C_i} - \frac{P_i C_i}{1+P_i C_i} (j\omega_k)] \approx 0.1$$

for the maximum achievable bandwidth, $11.2\, rad/s$;

- the transfer function $\frac{G_1}{1+G_1 C_{IMC}}$ has a maximum gain of approximately 10 dB since in the algorithm of (Lee *et al.*, 1995) there was nothing limiting this gain but our method gives $\bar{\sigma}[\frac{P_i}{1+P_i C_i}] \simeq 6.8\, dB$;
- both $\frac{C_{IMC}}{1+G_1 C_{IMC}}$ of (Lee *et al.*, 1995) and our $\frac{C_i}{1+P_i C_i}$ had a gain less than 30 dB and hence with respect to this criterion, both designs were satisfactory;
- for the design of (Lee *et al.*, 1995),

  $$\max_{1\leq k\leq N} \bar{\sigma}[H(P_t, C_{IMC}) - H(G_1, C_{IMC})\ (j\omega_k)] = 2.1530$$

  whereas in our algorithm

  $$\max_{1\leq k\leq N} \bar{\sigma}[H(P_t, C_{final}) - H(P_3, C_{final})\ (j\omega_k)] = 0.257\,.$$

  This shows that the final controller of (Lee *et al.*, 1995) performs differently in a closed-loop sense on P_t than on G_1. The difference in closed-loop transfer functions of our final controller on P_t and on P_3 is well contained.

These points assert the superiority of our algorithm compared to the one of (Lee *et al.*, 1995) in terms of keeping $\frac{P_t C_i}{1+P_t C_i}$ close to $\frac{P_i C_i}{1+P_i C_i}$, limiting the size of $\frac{P_i}{1+P_i C_i}$ and $\frac{C_i}{1+P_t C_i}$, and ensuring that the flags γ_i and $\max_{1\leq k\leq N} \bar{\sigma}[H(P_t, C_i) - H(P_i, C_i)\ (j\omega_k)]$ are easy to handle.

5. CONCLUSION

This paper has introduced a modified algorithm for the windsurfer approach to iterative identification and control by incorporating a new controller design method. This $\mathcal{H}_\infty$ controller design method can be applied when the plant is stable or unstable, or has $j\omega$-axis zeros. Additionally, it is well capable of dealing with plants with lightly-damped poles and zeros and situations where the bandwidth of F_i is orders of magnitude greater than that of P_i. This algorithm also provides us with one number, γ_i, that easily flags whether the desired performance specifications have been achieved. Furthermore, an easy computation $\max_{1\leq k\leq N} \bar{\sigma}[H(P_t, C_i) - H(P_i, C_i)\ (j\omega_k)]$indicates whether re-identification is necessary or not. An extension of this research is currently underway to make the 10% bandwidth expansion rule discussed in Step 6 of the proposed algorithm more automatic and less empirical.

REFERENCES

Anderson, B. D. O. (2002). Windsurfing approach to iterative control design. In: *Iterative Identification and Control* (P. Albertos and A. Sala, Eds.). pp. 143–166. Springer-Verlag, London.

Anderson, B. D. O. and R. L. Kosut (1991). Adaptive robust control: on-line learning. In: *Proceedings of the 30th IEEE Conference on Decision and Control*. Brighton, UK. pp. 297–298.

Campi, M., W. S. Lee and B. D. O. Anderson (1982). New filters for internal model control design. *International Journal of Robust and Nonlinear Control* **4**, 757–775.

Hansen, F. R. (1989). A fractional representation approach to closed-loop system identification and experiment design. PhD thesis. Standford University. USA.

Lee, W. S., B. D. O. Anderson, I. M. Y. Mareels and R. L. Kosut (1995). On some key issues in the windsurfer approach to adaptive robust control. *Automatica* **31**, 1619–1636.

Lee, W. S., B. D. O. Anderson, R. L. Kosut and I. M. Y. Mareels (1993). A new approach to adaptive robust control. *International Journal of Adaptive Control and Signal Processing* **7**, 183–211.

Lee, W. S., I. M. Y. Mareels and B. D. O. Anderson (2001). Iterative identification and two step control design for partially unknown unstable plants. *International Journal of Control* **74**(1), 43–57.

Morari, M. and E. Zafiriou (1989). *Robust Process Control*. Prentice-Hall, Englewood Cliffs, NJ.

Obinata, G. and B. D. O. Anderson (2001). *Model Reduction for Control System Design*. Springer-Verlag, Berlin.

Vinnicombe, G. (2000). *Uncertainty and Feedback: H_∞ loop-shaping and the ν-gap metric*. Imperial College Press.

Zhou, K., J. C. Doyle and K. Glover (1996). *Robust and Optimal Control*. Prentice-Hall, Inc.